International Journal of Precision Engineering and Manufacturing (2021) 22:1323–1334
https://doi.org/10.1007/s12541-021-00519-9

Online ISSN 2005-4602
Print ISSN 2234-7593

REGULAR PAPER

# Biomechanical Role of Nucleotomy in Vibration Characteristics of Human Spine

**Qing-Dong Wang**[1] · **Li-Xin Guo**[1]

Received: 22 June 2020 / Revised: 19 March 2021 / Accepted: 30 March 2021 / Published online: 26 May 2021


**Abstract**
Nucleotomy is a common surgical procedure for the treatment of lumbar diseases. It may accelerate degeneration in the operated disc and decreased segmental stability, and this has been widely concerned by scholars for many years. However, under whole-body vibration, nucleotomy how to affect the vibration characteristics of the lumbar spine and complications is urgent to know. A three-dimensional nonlinear osteoligamentous finite element model of the intact L1-sacrum lumbar spine with muscles was established, and the nucleus of the L4–L5 disc was removed in the nucleotomy model. The lower surface of the sacrum was fully constrained for all models. A 5 Hz, 40 N sinusoidal vertical load supplemented with a 400 N preload was applied at L1 to simulate the vertical vibration of the human body. The results showed that nucleotomy increased the dynamic responses of the discs such as stress in the annulus ground substance and intradiscal pressure both in the maximum value and vibration amplitude. The maximum endplate stresses and corresponding vibration amplitudes of the denucleated L4–L5 level increased because of nucleotomy. Nucleotomy decreased the maximum response values of disc height and segmental lordosis but increased the corresponding amplitudes. Therefore, these findings imply that nucleotomy may increase the risk of developing complications such as disc degeneration, adjacent segment disease, endplate degeneration, lumbar instability, nerve root compress, isthmic spondylolisthesis, and lumbar disc herniation under whole-body vibration. This study reveals insights into the effect of the nucleotomy on the vibration characteristics of the lumbar spine and provides new information toward the relationship between nucleotomy and complications.

**Keywords** Whole-body vibration · Nucleotomy · Lumbar spine · Complication · Finite element

## 1 Introduction

Disc degeneration is one of the most common causes of low-back pain and disorders [1]. One of the main manifestations of disc degeneration is the loss of the nucleus pulposus. Some researchers have reported that the volume loss of the nucleus resulting from decreased proteoglycan and water concentration leads to early disc degeneration [2]. The alteration of the nucleus affect the lumbar disc mechanical behavior directly. However, to treat lumbar disc herniation and other lumbar diseases, nucleus pulposus has to be removed. This operation is called nucleotomy. The nucleotomy may change the biomechanical characteristics of the lumbar, such as the intradiscal pressure (IDP), the stress distributions in the annulus fibrosus, and the endplate stress. So it contributes to the degradation, disc prolapse, and low back disorders [3, 4].

There have been some valuable researches on the effects of the nucleus removal on the biomechanical properties of the lumbar spine. A clinical study by Dunlop et al. [5] showed that the pressure across the facet joints increased when the nucleus was removed. O'Connell et al. [6] concluded that nucleotomy altered the internal radial and axial strains of the annulus fibrosus under compressive load in the neutral position, which might lead to its damage and microfractures. The research by Adams et al. [7] reported that when 17% of the intervertebral discs protrude, 58% of the vertebral endplates have ruptured. Some studies concluded that nucleotomy increased disc displacement and decreased segmental stability [4, 8]. Although many scholars have provided valuable experimental and numerical results for us to understand the effects of nucleotomy on biomechanical properties of the lumbar spine, most of the studies were

✉ Li-Xin Guo
lxguo@mail.neu.edu.cn

[1] School of Mechanical Engineering and Automation, Northeastern University, Shenyang 110819, China

carried out under the static loads and without taking into account whole-body vibration (WBV). In other words, few studies focus on the effects of nucleotomy on the vibration characteristics of the lumbar spine under vibration.

The whole-body vibration typically presenting in vehicles resulted in spinal disorders [9], low back pain [10], intervertebral disc injuries [11], sciatic pain [12], and other lumbar diseases. Whether clinical, experimental results or numerous studies have reported that vibration loads produced significant increases in stresses, intradiscal pressure, displacement, and degenerative changes in the spine, as compared to the static loads [13, 14]. In daily life, the whole-body vibration such as driving a car or taking a bus is very common but inevitable. Therefore, the vibration characteristics of the lumbar spine under vibration after nucleotomy have deserved more attention. Edward et al. found that the cyclic loading resulted in significant and large changes to both the stiffness and stress relaxation behaviors [15]. A finite element (FE) study by Fan et al. investigated the effect of nucleus removal on the biomechanical properties of the lumbar spine under vibration and found that the nucleus removal increased the dynamic responses such as stress in annulus ground substance and intradiscal pressure at all disc levels under the axial cyclic loading [16].

Although these previous studies have given valuable insights into the effects of nucleotomy on the lumbar spine under the cyclic loading, the employed FE models did not take into account the muscles. The effect of the nucleotomy on the endplates was also not taken into account. The purpose of this study was to investigate the effects of nucleotomy on the vibration characteristics of the lumbar spine using a FE model of L1–sacrum segments with 5 muscle groups, including the effects on the discs and the L4, 5 endplates, especially regarding complications such as adjacent segment disease (ASD), disc degeneration, endplate degeneration, lumbar instability, and lumbar disc herniation.

## 2 Materials and Methods

### 2.1 FE Modeling

A three-dimensional nonlinear osteoligamentous FE model of the intact L1-sacrum lumbar spine was established in this study [17, 18]. The geometry of the spine was obtained by computer scanning tomographic specimens. The intact model consists of vertebrae, endplates, intervertebral discs, posterior bony elements, various ligaments, and muscles (Fig. 1). Each vertebral body consists of the outer 0.5–1.0 mm cortical bone and the inner cancellous bone. Intervertebral disc is composed of annular matrix, annulus fibrosus, and nucleus pulposus. The 0.5 mm endplate is between the vertebral body and the intervertebral disc. The annulus ground substance (AGS), consisting of six fiber layers, encloses the nucleus pulposus. The Young's modulus of the fiber ring decreases proportionally from the outer layer to the inner layer. The ligaments include the anterior longitudinal ligament, posterior longitudinal ligament, supraspinous ligament, interspinous ligament, intertransverse ligament, ligamentum flavum, and capsular ligament. The lumbar

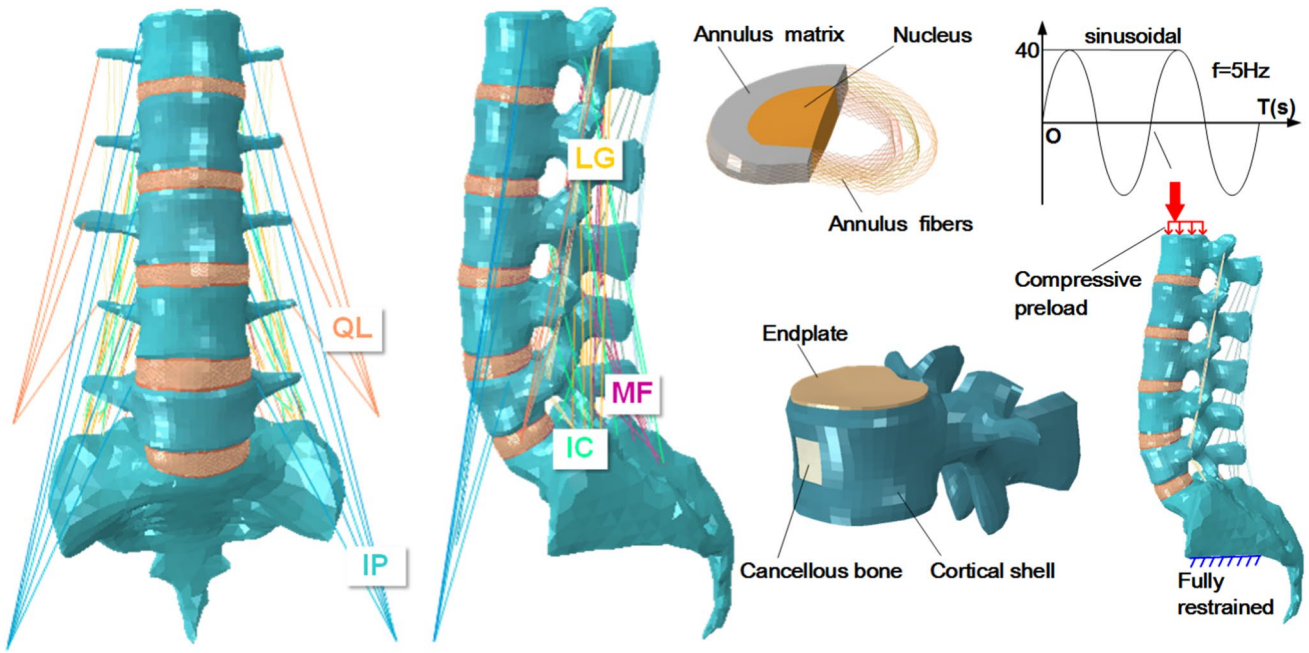


**Fig. 1** A nonlinear lumbar model with muscle groups

ligaments are active in tension only. Surface-to-surface contact conditions were applied for the interfaces of facet joints. The material properties were assumed to be homogeneous and isotropic, the corresponding data were given in Table 1 [19–23].

The nucleus of the L4-L5 disc was removed to simulate the removal of the nucleus in the nucleotomy model. The reason for choosing this level is that its prevalence in individuals suffering from lumbar diseases is greater than other intervertebral discs [24, 25].

## 2.2 Boundary and Loading Conditions

In this study, when a person in a sitting posture was exposed to vertical vibration, the load on lumbar spine were the compression load caused by upper body weight and muscle contraction and the dynamic load caused by upper body mass under vibration condition. To simulate the physiological compression load of lumbar spine, a "muscle mode" was used to apply the load. The mechanical effects of abdominal and local muscles, as well as the effect of upper body weight, were included in this study. The local muscles in this study were identical to those in the study by Shirazi-Adl et al. [26] The muscle groups include quadrates lumborum (QL), iliocostalis (IC), longissimus (LG), iliopsoas (IP), and multifidus (MF). The coordinate, the origin site, and the insertion site of the left and right muscles are symmetrical to the sagittal plane. There are 46 muscles in the present model. The operation method was cited from the literature studies [27, 28].

The physiological compression load of the whole lumbar spine caused by abdominal muscle contraction and the upper body weight is represented by a 400 N compressive preload applied at the superior surface of L1 [29, 30]. When a person was in a sitting posture, the load on the lumbar spine was mainly borne by the lumbar vertebrae and the intervertebral disc, and the lumbar muscles only play the role of maintaining lumbar balance. Relevant literature found that the lumbar muscles were relatively relaxed at this time, and the muscle activity was small [26]. The contractions of the 5 muscular groups were along the lumbar column to stabilize the lumbosacral column [27]. The forces of muscles were cited in the literature studies, and some published studies have adopted this loading mode [26, 27, 31], the corresponding data were given in Table 2.

Meanwhile, a 5 Hz, 40 N sinusoidal vertical load, which is considered to be the main cause of human vibration in many vehicle transportations [13, 32], was applied to the upper surface of L1 to simulate the vertical vibration of the human body. A 40 kg mass point was designated to the top of L1 to simulate the effect of body mass on the lumbar spine [33–35]. The lower surface of the sacrum was fully constrained for all models in all directions throughout the simulation process. In this study, the accuracy of the grid has been verified. The element geometry adopted in this model completely met the elements' quality criteria [36]. Abaqus 6.14(Dassault Systemes Simulia Corp) was used to analyze

**Table 1** Material properties of the finite element model

| Component | Element type | Young's Modulus (MPa) | Poisson's Ratio | Density (e-6 kg/mm$^3$) | Cross-sectional Area (mm$^2$) |
|---|---|---|---|---|---|
| *Bone* | | | | | |
| Cancellous bone | C3D4 | 100 | 0.2 | 1.1 | |
| Cortical bone | C3D8 | 12,000 | 0.3 | 1.7 | |
| Posterior bone | C3D4 | 3500 | 0.25 | 1.4 | |
| Endplate | C3D8 | 500 | 0.25 | 1.2 | |
| *Intervertebral disc* | | | | | |
| Nucleus pulposus | C3D8 | 1 | 0.49 | 1.02 | |
| Annulus ground substance | C3D8 | 4.2 | 0.45 | 1.05 | |
| Annulus fibers | T3D2 | 357–550 | 0.3 | 1.0 | |
| *Ligaments* | | | | | |
| Anterior longitudinal | T3D2 | 7.8(< 12.0%) 20.0(> 12.0%) | | 1.0 | 63.7 |
| Posterior longitudinal | T3D2 | 10.0 (< 11.0%) 20.0 (> 11.0%) | | 1.0 | 20 |
| Capsular | T3D2 | 7.5(< 25.0%) 32.9 (> 25.0%) | | 1.0 | 30 |
| Intertransverse | T3D2 | 10.0(< 18.0%) 58.7 (> 18.0%) | | 1.0 | 1.8 |
| Interspinous | T3D2 | 10.0 (< 14.0%) 11.6 (> 14.0%) | | 1.0 | 40 |
| Supraspinous | T3D2 | 8.0 (< 20.0%) 15 (> 20.0%) | | 1.0 | 30 |
| Ligamentum flavum | T3D2 | 15.0 (< 6.2%) 19.5 (> 6.2%) | | 1.0 | 40 |

**Table 2** Forces of the 5 Muscle Groups at the Different Levels

| IP Muscle Group | | MF Muscle Group | | LG Muscle Group | | IC Muscle Group | | QL Muscle Group | |
|---|---|---|---|---|---|---|---|---|---|
| Vertebral Level | Muscle Force (N) | Vertebral Level | Muscle Force (N) | Vertebral Level | Muscle Force (N) | Vertebral Level | Muscle Force (N) | Vertebral Level | Muscle Force (N) |
| L1 | 1.3 | L1 | 11.2 | L1 | 0.1 | L1 | 10.0 | L1 | 0.2 |
| L2 | 0.5 | L2 | 11.1 | L2 | 0.1 | L2 | 12.3 | L2 | 1.0 |
| L3 | 5.8 | L3 | 9.2 | L3 | 1.1 | L3 | 15.6 | L3 | 1.1 |
| L4 | 13.5 | L4 | 0.0 | L4 | 50.6 | L4 | 86.9 | L4 | 0.0 |
| L5 | 10.0 | L5 | 6.9 | L5 | 53.4 | – | – | – | – |

the stress in AGS, the IDP, the displacement of disc, segmental lordosis, disc height, the stress in endplates of the denucleated L4–L5 level. The results were periodic, and a more representative period of 0–1.0 s was chosen from the entire vibration process (2 s) in this study.

## 3 Results

### 3.1 Validation of the FE Model

In this paper, based on the existing in vitro cadaveric experiments and numerical analysis, the L1-sacrum spine FE model was verified. Renner et al. [37] presented the compressive deformation of the lumbar spine under 1200 N follower load, the range of motion of the lumbar spine under the flexion and extension moments of 8 and 6 Nm, respectively, with 800 N follower load, and the range of motion of the lumbar spine under ± 6Nm left–right lateral bending moment. Dreischarf et al. [38] presented IDP of the lumbar spine under 7.5 Nm flexion moment with 1175 N follower load, 7.5 Nm extension follower load with 500 N follower load, and 7.8 Nm lateral bending moment with 700 N follower load. The present model results were in good agreement with these published results. The developed model can be used for further analysis. The detailed model verification results are shown in Table 3.

### 3.2 Effect of Nucleotomy on the Intervertebral Discs

For the intervertebral discs, the IDP, Von-Mises stress in the annulus, and displacement were assumed to be the average values in the elements. It was observed in Fig. 2 that the nucleotomy model increased the maximum values and

**Table 3** Comparison of the results for the present study with the experimental data of Renner et al. [37] and numerical results of Dreischarf et al. [38] under static loading conditions

| Loading condition | Chosen parameters | Spinal levels | | | |
|---|---|---|---|---|---|
| | | L1-L2 | L2-L3 | L3-L4 | L4-L5 |
| *1200 N FL* | | | | | |
| Renner et al | Compression (mm) | 1.20 ± 0.30 | 1.50 ± 0.80 | 1.50 ± 0.50 | 1.6 0 ± 0.50 |
| Present study | Compression (mm) | 1.13 | 1.37 | 1.55 | 1.43 |
| *+ 8/-6 Nm FLX-EXT with 800 N FL* | | | | | |
| Renner et al | Segmental ROM (deg) | 5.7 ± 2.7 | 6.4 ± 1.5 | 8.30 ± 2.1 | 10.0 ± 2.8 |
| Present study | Segmental ROM (deg) | 4.33 | 4.97 | 6.15 | 7.33 |
| *± 6 Nm left–right LAT* | | | | | |
| Renner et al | Segmental ROM (deg) | 10.5 ± 5.6 | 12.3 ± 6.7 | 8.4 ± 2.9 | 10.0 ± 3.0 |
| Present study | Segmental ROM (deg) | 10.1 | 8.53 | 6.32 | 8.45 |
| *7.5 Nm FLX with 1175 N FL* | | | | | |
| Dreischarf et al | Intradiscal pressure (MPa) | 1.8 ± 0.1 | 1.5 ± 0.4 | 1.3 ± 0.3 | 1.3 ± 0.3 |
| Present study | Intradiscal pressure (MPa) | 1.72 | 1.63 | 1.43 | 1.42 |
| *7.5 Nm EXT with 500 N FL* | | | | | |
| Dreischarf et al | Intradiscal pressure (MPa) | 0.6 ± 0.4 | 0.5 ± 0.3 | 0.5 ± 0.4 | 0.5 ± 0.4 |
| Present study | Intradiscal pressure (MPa) | 0.49 | 0.66 | 0.69 | 0.73 |
| *7.8 Nm LAT with 700 N FL* | | | | | |
| Dreischarf et al | Intradiscal pressure (MPa) | 0.7 ± 0.3 | 0.7 ± 0.4 | 0.6 ± 0.3 | 0.6 ± 0.4 |
| Present study | Intradiscal pressure (MPa) | 0.58 | 1.04 | 0.83 | 0.89 |

*FLX*, flexion; *EXT*, extension; *LAT*, lateral bending; *FL*, follower load; *ROM*, range of motion

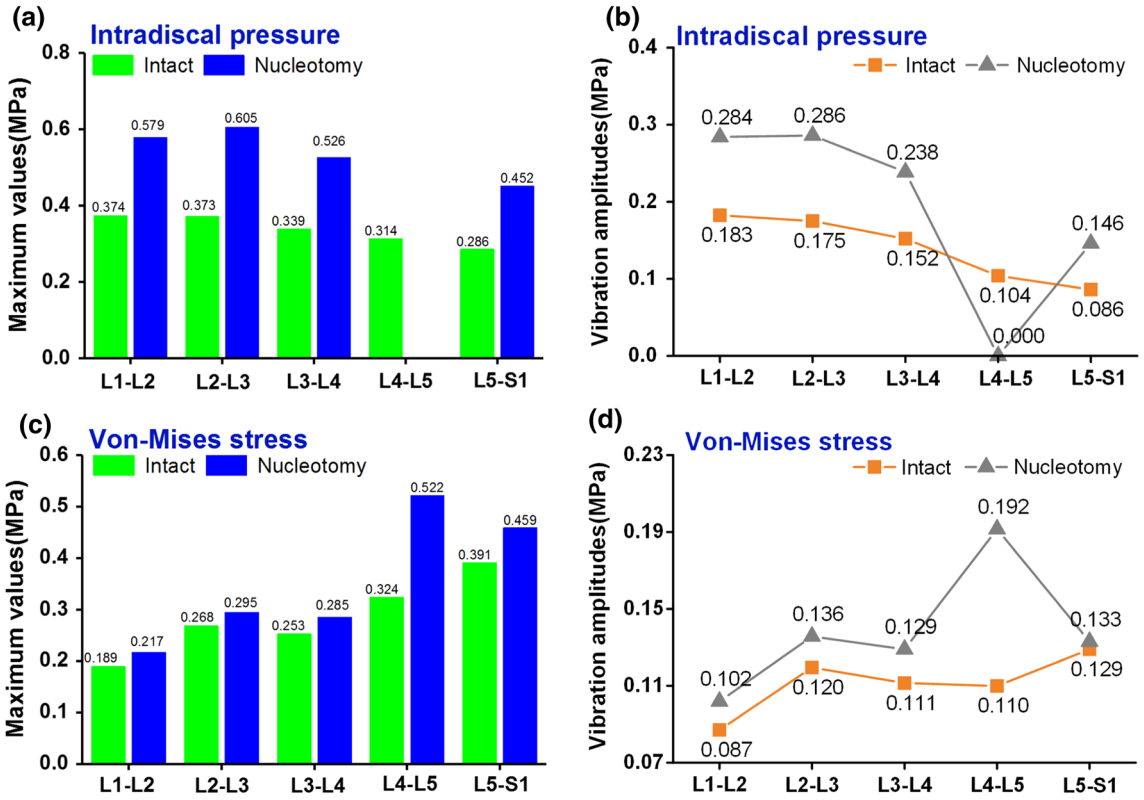


**Fig. 2** The dynamic responses of the discs. **a** Maximum values of the stress in AGS **b** Vibration amplitudes of the stress in AGS **c** Maximum values of the IDP **d** Vibration amplitudes of the IDP

the amplitudes of the stress in AGS and IDP. The most significant increase was at the denucleated L4–L5 level. The maximum value of the stress in AGS increased from 0.324 to 0.522 MPa, and the vibration amplitude increased from 0.101 to 0.191 MPa. The displacement is the main index to reflect the stability of the lumbar. It was found from the displacement nephogram of the intact and nucleotomy models (Fig. 3a, b) that nucleotomy increased the high-displacement region both in the anterior–posterior (A–P) and the axial displacement. The displacement nephogram of the discs showed that the nucleotomy model increased the high-displacement region in the A-P and axial displacement compared with the intact model (Fig. 3c, d).

It was observed in Fig. 4 that the nucleotomy model increased the maximum A-P and axial displacement of L1–L2, L2–L3, and L3–L4 discs. For example, the A-P displacement of L1–L2, L2–L3, and L3–L4 discs were 5.38, 3.19, and 1.25 mm for the intact model, 5.63, 3.34, and 1.27 mm for the nucleotomy model. The axial displacement of the L1–L2, L2-L3, and L3–L4 discs were − 3.47, -2.6, and -1.88 mm for the intact model, − 3.74, − 2.9, and − 2.21 mm for the nucleotomy model. The "-" indicates the displacement direction. The A-P and axial displacement amplitudes of the L1–L2 and L2–L3 discs were increased (A–P: 0.044 and 0.144 mm for the intact model, 0.075 and 0.156 mm for the nucleotomy model; Axial: 0.056 and 0.457 mm for the intact model, 0.631 and 0.522 mm for the nucleotomy model).

### 3.3 Effect of Nucleotomy on the Endplates of the Denucleated level (L4-L5)

The intervertebral disc and endplate interact with each other. The endplates of the denucleated level were very vulnerable to injury because of the nucleus removal. The dynamic response of the stress in the L4–L5 endplates indicated that the nucleotomy model increased the endplate stress during the entire vibration simulation process compared to the intact model (Fig. 5a, b). The maximum stresses in the L4 inferior endplate of the nucleotomy and intact model were 0.298 and 0.246 MPa, and these in the L5 superior endplate were 0.295 and 0.262 MPa (Fig. 5c). Similarly, the vibration amplitudes of the L4–L5 endplates stresses in the nucleotomy model were greater than these in the intact model. The vibration amplitudes of the L4–L5 endplates were 0.049, 0.054 MPa for the nucleotomy model, and 0.042, 0.046 MPa for the intact model (Fig. 5d).

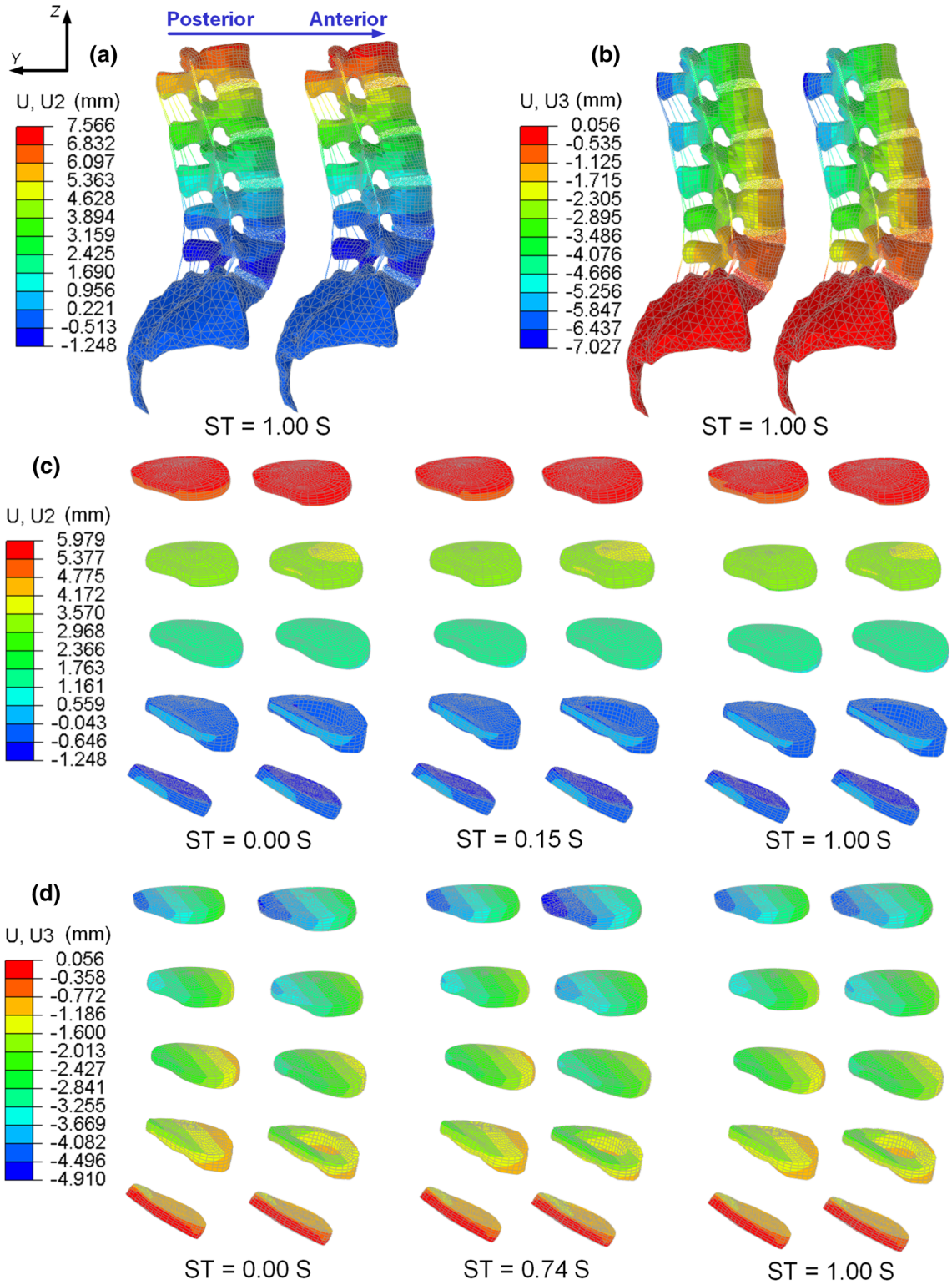


**Fig. 3** The displacement distributions of the lumbar and disc (Left: the intact model, Right: the nucleotomy model) **a** A–P displacement distributions of the lumbar model in the intact and nucleotomy model **b** Axial displacement distributions of the lumbar model in the intact and nucleotomy model **c** A–P displacement distributions of the discs in the intact and nucleotomy model when the step time (ST) was 0.00, 0.15, and 1.00 s **d** Axial displacement distributions of the discs in the intact and nucleotomy model when the step time (ST) was 0.00, 0.74, and 1.00 s

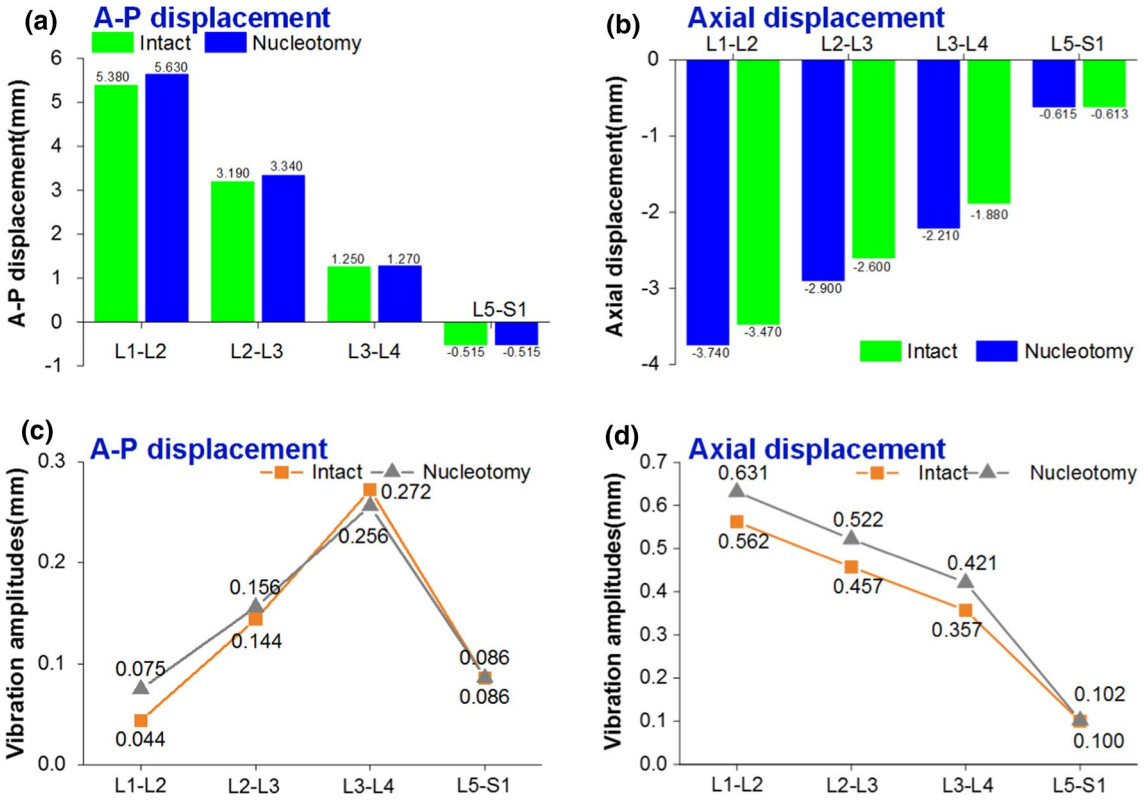


**Fig. 4** **a** Maximum values of the A–P displacement **b** Maximum values of the axial displacement **c** Vibration amplitudes of the A-P displacement **d** Vibration amplitudes of the axial displacement

### 3.4 Effect of Nucleotomy on the Disc Height and Segmental Lordosis at the Denucleated L4–L5 Level

The disc height and segmental lordosis are essential indexes reflecting the performance of lumbar and related to complications. A disc height measurement method (Fig. 6a) as reported by Drain et al. [39] was adopted in this study. Segmental lordosis was only measured at the denucleated L4-L5 level. It was found in Fig. 6 that nucleotomy decreased the disc height and segmental lordosis during the entire vibration process. The nucleotomy model decreased the maximum values of the disc height and segmental lordosis compared with the intact model. However, it increased their vibration amplitudes. The maximum disc height and the vibration amplitude was 0.3046, 0.0035 for the intact model, and 0.2957, 0.0054 for the nucleotomy model. The maximum segmental lordosis and the vibration amplitude, were 15.69°, 0.09° for the intact model, and 15.60°, 0.11° for the nucleotomy model.

## 4 Discussion

The effects of nucleotomy on the lumbar spine have been widely investigated, but most researches were only under the static load. The studies on the dynamic characteristics of the nucleotomy lumbar spine were rare and without taking into account the muscle. Therefore, this study researched the effects of nucleotomy on the vibration characteristics of the lumbar spine using a non-linear L1–L5 lumbar spine FE model with 5 muscle groups to investigate the relationship between nucleotomy and complications under the WBV. The dynamic characteristics of the lumbar spine such as IDP, the stress in AGS, disc displacement, and endplate stress were analyzed in this study. Some essential indexes related to complications were analyzed as well.

It is universally acknowledged that WBV may increase the risk of lumbar spine injury compared with static load. Nucleotomy decreased the strength and stability of the lumbar spine a relatively fragile and neuro sensitive site. The nucleotomy lumbar spine is more affected by the vibration. The vibration mode (a vertical sinusoidal vibration load of

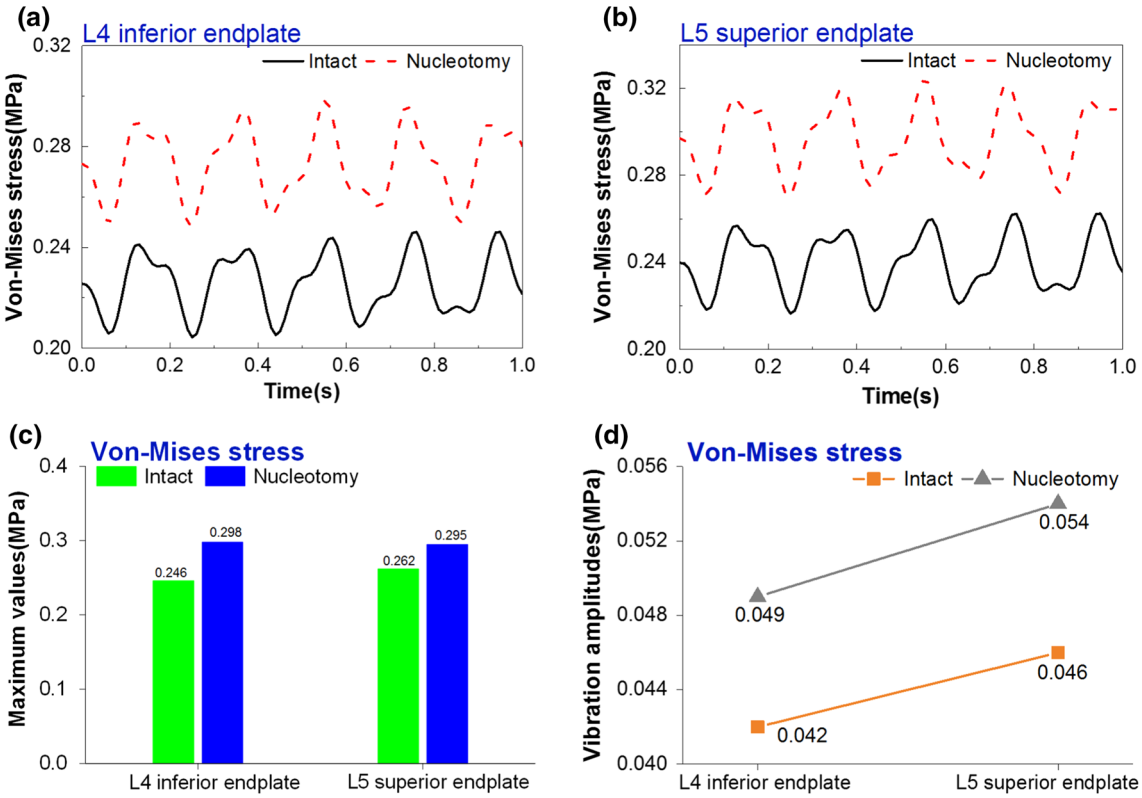


**Fig. 5** Dynamic response of the von-Mises stress in **a** L4 inferior endplate and **b** L5 superior endplate for the models. **c** Maximum values of the Von-Mises stress **d** Vibration amplitudes of the Von-Mises stress

40 N, 5 Hz) cited from some published studies was used in this study [13, 40].

It was demonstrated that the high stresses and strains might exacerbate the degeneration of spinal components and lead to various spinal disorders [41, 42]. The dynamic characteristics of the discs showed that the nulceotomy increased maximum values and vibration amplitudes of the IDP and stresses at all disc levels, especially the denucleated level (L4–L5). A FE study predicted the same trend that the nucleotomy increased dynamic responses of strain and stress to the vertical vibration load at the denucleated and the adjacent lumbar discs [17]. Moreover, for the L1–L3 adjacent discs, the nucleotomy increased not only the maximum values of the A–P and axial displacement but also their amplitudes. The results were consistent with the research of Frank et al. [8]. They reported that the nucleotomy increased the disc displacement, whereas the displacement zenith migrated posterolaterally. The analysis is as follows. The load was shared by the whole lumbar spine, vertebral bodies, and intervertebral discs, as shown in Fig. 7. The nucleotomy decreased the strength of the L4-L5 disc. The denucleated L4-L5 disc generated a greater dynamic response under vibration. The discs were the buffer areas for the vibration energy. The ability of the denucleated L4–L5 disc withstanding vibration energy is reduced. The vibration energy shared by the other discs (L1–L2, L2–L3, L3–L4, and L5–S1 discs) were increased in the nucleotomy model. These findings imply that the nucleotomy may increase the risk of ASD, disc degeneration, and lumbar disc herniation under WBV.

There was a high direct correlation between the endplate and the disc, and they interact with each other [43]. The research by Gruber et al. [44] reported that the sites of prominent disc degeneration evident on radiographs, the proportion of abnormalities in surface smoothness, margin irregularity, and endplate thickening were all statistically significant. In the current research, the nucleotomy model increased the L4 inferior and L5 superior endplate stresses during the entire simulation process compared to the intact model. The amplitudes of the L4 inferior and L5 superior endplate stresses were higher in the nucleotomy model than in the intact model. This result was consistent with the research of Zhu et al. [45] that removing the nucleus may increase the stress at the interface between disc and vertebra. Based on our results, we believe that nucleotomy may increase the risk of endplate degeneration or injury.

Loss of disc height and lordosis may result in some complications, such as low back pain, nerve root compress, ASD,

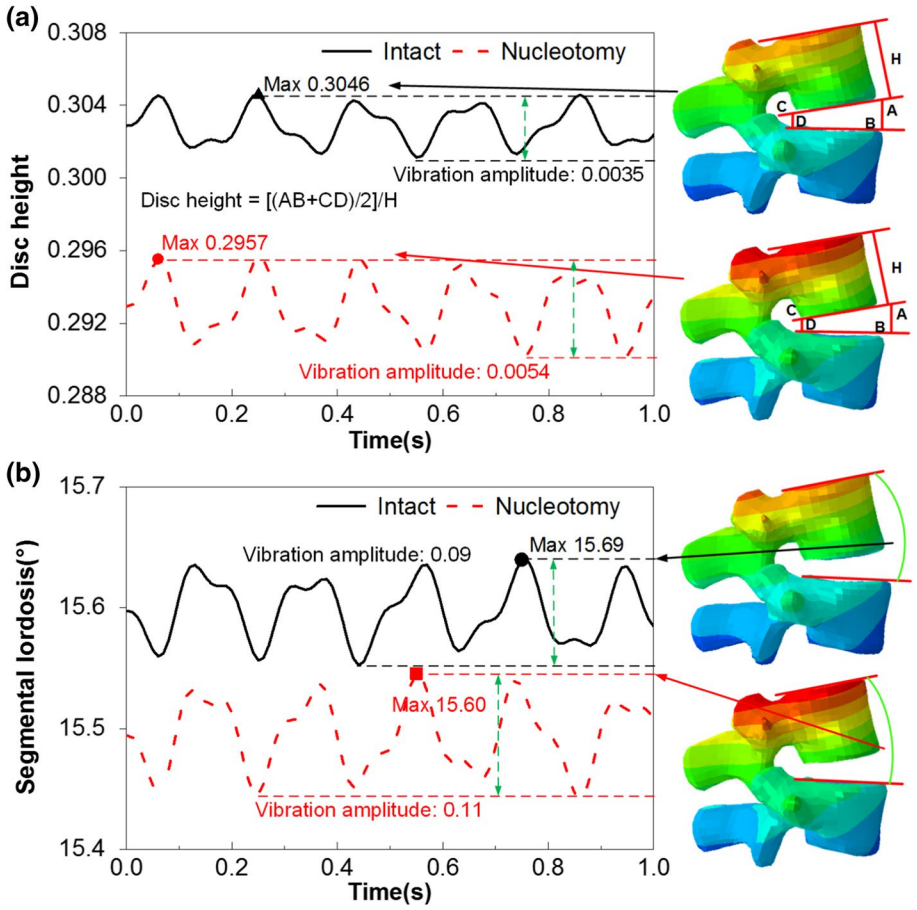


**Fig. 6** The dynamic response of **a** disc height and **b** segmental lordosis at L4–L5 denucleated level for models. Segmental lordosis: the angle represented by green arc

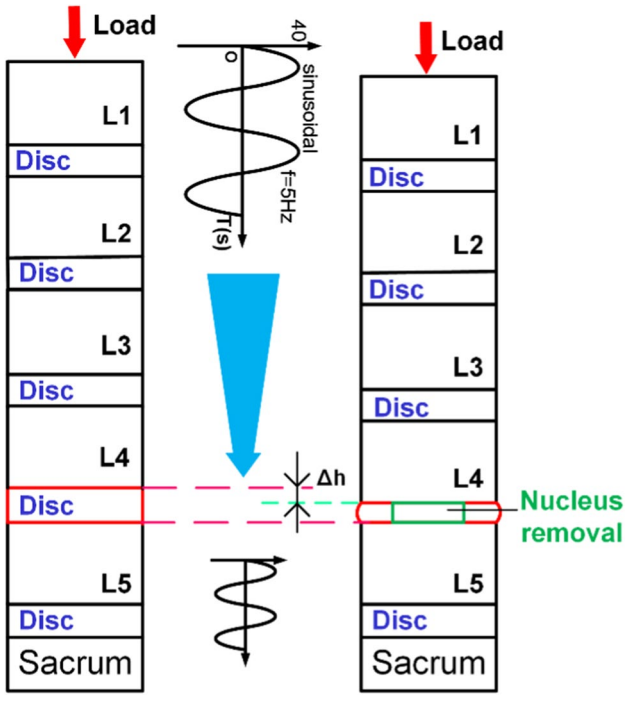


**Fig. 7** The schematic diagrams to illustrate the load-transferring mechanism of the intact and nucleotomy models at the denucleated (L4–L5) level

and isthmic spondylolisthesis [46–48]. The maximum disc height and segmental lordosis of the nucleotomy model during the vibration simulation process were lower than the intact model. The corresponding vibration amplitudes were higher in the nucleotomy than in the intact model. Some studies predicted the same trends for the nucleotomy using clinical analysis. They found that the nucleotomy may result in decreased disc height under the axial compression [3, 49]. When the load was on the top of the L1, there was the height difference (Δh) between the nucleotomy model and the intact model, as shown in Fig. 7. The stiffness of the L4-L5 disc was reduced because of the nucleotomy. So the nucleotomy model was prone to lumbar instability and exhibited a higher dynamic response (as the results illustrated). Based on our findings, we believe that the nucleotomy model may cause lumbar instability and have a higher risk of developing complications such as nerve root compress, ASD, and isthmic spondylolisthesis during WBV.

There are some potential limitations inherent in this study. The material properties, including non-linear behavior of the spinal ligaments, degenerative changes caused by osteophytes, and sclerosis may be neglected. But the neglected details had little effect on the spine. And our results were consistent with the in vitro experiments confirm the reality

of our spine FE model. A 400 N pressure preload applied to the model cannot entirely replace the complex contribution of abdominal muscle and the upper body weight to the spine. In this study, we focus on the dynamic characteristics of the lumbar spine under vertical vibration. Therefore, we ignore the mass distribution of the upper body and adopt a mass point on the spine model to simulate the human body mass.

## 5 Conclusions

The effects of nucleotomy on the vibration characteristics of the lumbar spine were studied to analyze the relationship between nucleotomy and complications under WBV. The results showed that nucleotomy may increase the risk of developing complications such as disc degeneration, ASD, endplate degeneration, lumbar instability, nerve root compress, isthmic spondylolisthesis, and lumbar disc herniation under WBV. This study reveals insights into the effect of the nucleotomy on the vibration characteristics of the lumbar spine and provides new information toward the relationship between nucleotomy and complications.

**Acknowledgements** This work was supported by the National Natural Science Foundation of China (51875096).

### Declarations

**Conflict of interest** The authors declared that they have no conflict of interest.

## References

1. Vaccaro, A. R. (2005). *Spine: Core knowledge in orthopaedics*. . Mosby Publishing.
2. Buckwalter, J. A. (1995). Spine update: Aging and degeneration of the human intervertebral disc. *Spine, 20*(11), 1307–1314.
3. Cannella, M., Isaacs, J. L., Allen, S., Orana, A., Vresilovic, E., & Marcolongo, M. (2014). Nucleus implantation: The biomechanics of augmentation versus replacement with varying degrees of nucleotomy. *Journal of Biomechanical Engineering, 136*(5), 051001.
4. Van Ooij, A., Oner, F. C., & Verbout, A. J. (2003). Complications of artificial disc replacement. *Journal of Spinal Disorders & Techniques, 16*(4), 369–383.
5. Dunlop, R., Adams, M., & Hutton, W. (1984). Disc space narrowing and the lumbar facet joints. *The Journal of Bone and Joint Surgery, British, 66-B*(5), 706–710.
6. O'Connell, G. D., Malhotra, N. R., Vresilovic, E. J., & Elliott, D. M. (2011). The effect of nucleotomy and the dependence of degeneration of human intervertebral disc strain in axial compression. *Spine, 36*(21), 1765–1771.
7. Adams, M. A., & Hutton, W. C. (1985). Gradual disc prolapse. *Spine, 10*(6), 524–531.
8. Heuer, F., Schmidt, H., Claes, L., & Wilke, H.-J. (2008). A new laser scanning technique for imaging intervertebral disc displacement and its application to modeling nucleotomy. *Clinical Biomechanics, 23*(3), 260–269.
9. Choi, H. W., Kim, Y. E., & Chae, S. W. (2016). Effects of the level of mono-segmental dynamic stabilization on the whole lumbar spine. *International Journal of Precision Engineering and Manufacturing, 17*(5), 603–611.
10. Bovenzi, M., Schust, M., & Mauro, M. (2017). An overview of low back pain and occupational exposures to whole-body vibration and mechanical shocks. *La Medicina Del Lavoro, 108*(6), 419–433.
11. Griffin, M. J., & Erdreich, J. (1990). Handbook of human vibration. *Journal of the Acoustical Society of America, 4*, 2213.
12. Burström, L., Nilsson, T., & Wahlström, J. (2014). Whole-body vibration and the risk of low back pain and sciatica: A systematic review and meta-analysis. *International Archives of Occupational and Environmental Health, 88*(4), 403–418.
13. Goel, V. K. (1994). Investigation of vibration characteristics of the ligamentous lumbar spine using the finite element approach. *Journal of Biomechanical Engineering, 116*(4), 377–83.
14. Wilke, H.-J., Kaiser, D., Volkheimer, D., Hackenbroch, C., Püschel, K., & Rauschmann, M. (2016). A pedicle screw system and a lamina hook system provide similar primary and long-term stability: A biomechanical in vitro study with quasi-static and dynamic loading conditions. *European Spine Journal, 25*(9), 2919–2928.
15. Vresilovic, E. J., Johannessen, W., & Elliott, D. M. (2006). Disc mechanics with trans-endplate partial nucleotomy are not fully restored following cyclic compressive loading and unloaded recovery. *Journal of Biomechanical Engineering, 128*(6), 823.
16. Fan, W., & Guo, L. X. (2018). Finite element investigation of the effect of nucleus removal on vibration characteristics of the lumbar spine under a compressive follower preload. *Journal of the Mechanical Behavior of Biomedical Materials, 78*, 342–351.
17. Fan, W., & Guo, L. X. (2018). Biomechanical comparison of nucleotomy with lumbar spine fusion versus nucleotomy alone: Vibration analysis of the adjacent spinal segments. *International Journal of Precision Engineering and Manufacturing, 19*(10), 1561–1568.
18. Guo, L. X., & Wang, Q. D. (2020). Biomechanical analysis of a new bilateral pedicle screw fixator system based on topological optimization. *International Journal of Precision Engineering and Manufacturing*. https://doi.org/10.1007/s12541-020-00336-6.
19. Goel, V. K., Mehta, A., Jangra, J., Faizan, A., Kiapour, A., Hoy, R. W., & Fauth, A. R. (2007). Anatomic facet replacement system (AFRS) restoration of lumbar segment mechanics to intact: A finite element study and in vitro cadaver investigation. *SAS Journal, 1*(1), 46–54.
20. Wu, H.-C., & Yao, R.-F. (1976). Mechanical behavior of the human annulus fibrosus. *Journal of Biomechanics, 9*(1), 1–7.
21. Kim, Y. H., Jung, T. G., Park, E. Y., Kang, G. W., Kim, K. A., & Lee, S. J. (2015). Biomechanical efficacy of a combined interspinous fusion system with a lumbar interbody fusion cage. *International Journal of Precision Engineering and Manufacturing, 16*(5), 997–1001.
22. Lim, J. W. (2018). Age-related stability for artificial disc fixators inserted into a lumbar vertebra: Finite element analysis. *International Journal of Precision Engineering and Manufacturing, 19*(2), 271–280.
23. Masni-Azian, & Tanaka, M. . (2018). Biomechanical investigation on the influence of the regional material degeneration of an intervertebral disc in a lower lumbar spinal unit: A finite element study. *Computers in Biology and Medicine, 98*, 26–38.
24. Cheung, K., Karppinen, J., Chan, D., Ho, D., Song, Y., Sham, P., Cheah, K. S. E., Leong, J. C. Y., & Luk, K. D. K. (2009). Prevalence and pattern of lumbar magnetic resonance imaging

changes in a population study of one thousand forty-three individuals. *Spine, 34*(9), 934–940.
25. Ruberté, L. M., Natarajan, R. N., & Andersson, G. B. (2009). Influence of single-level lumbar degenerative disc disease on the behavior of the adjacent segments-a finite element model study. *Journal of Biomechanics, 42*(3), 341–348.
26. Shirazi-Adl, A., Sadouk, S., Parnianpour, M., Pop, D., & El-Rich, M. (2002). Muscle force evaluation and the role of posture in human lumbar spine under compression. *European Spine Journal, 11*(6), 519–526.
27. Chuang, W.-H., Lin, S.-C., Chen, S.-H., Wang, C.-W., Tsai, W.-C., Chen, Y.-J., & Hwang, J.-R. (2012). Biomechanical Effects of Disc Degeneration and Hybrid Fixation on the Transition and Adjacent Lumbar Segments. *Spine, 37*(24), E1488–E1497.
28. Bazrgari, B., Shirazi-Adl, A., & Arjmand, N. (2006). Analysis of squat and stoop dynamic liftings: Muscle forces and internal spinal loads. *European Spine Journal, 16*(5), 687–699.
29. Chen, S.-H., Zhong, Z.-C., Chen, C.-S., Chen, W.-J., & Hung, C. (2009). Biomechanical comparison between lumbar disc arthroplasty and fusion. *Medical Engineering & Physics, 31*(2), 244–253.
30. Zhong, Z.-C., Chen, S.-H., & Hung, C.-H. (2008). Load- and displacement-controlled finite element analyses on fusion and non-fusion spinal implants. *Proceedings of the Institution of Mechanical Engineers, Part H: Journal of Engineering in Medicine, 223*(2), 143–157.
31. Chuang, W.-H., Kuo, Y.-J., Lin, S.-C., Wang, C.-W., Chen, S.-H., Chen, Y.-J., & Hwang, J.-R. (2013). Comparison among load-, ROM-, and displacement-controlled methods used in the lumbosacral nonlinear finite-element analysis. *Spine, 38*(5), E276–E285. https://doi.org/10.1097/brs.0b013e31828251f9.
32. Naveen, R. R., & Krishnapillai, S. (2020). An improved spinal injury parameter model for underbody impulsive loading scenarios. *International Journal for Numerical Methods in Biomedical Engineering, 36*(3), e3307.
33. Shirazi-Adl, A., & Parnianpour, M. (1996). Role of posture in mechanics of the lumbar spine in compression. *Journal of Spinal Disorders, 9*(4), 277–286.
34. Xu, M., Yang, J., Lieberman, I., & Haddas, R. (2017). Finite element method-based study for effect of adult degenerative scoliosis on the spinal vibration characteristics. *Computers in Biology and Medicine, 84*, 53–58.
35. Guo, L. X., Zhang, Y. M., & Zhang, M. (2011). Finite element modeling and modal analysis of the human spine vibration configuration. *IEEE Transactions on Biomedical Engineering, 58*(10), 2987–2990.
36. Tsouknidas, A., Savvakis, S., Asaniotis, Y., Anagnostidis, K., Lontos, A., & Michailidis, N. (2013). The effect of kyphoplasty parameters on the dynamic load transfer within the lumbar spine considering the response of a bio-realistic spine segment. *Clinical Biomechanics, 28*(9–10), 949–955.
37. Renner, S. M., Natarajan, R. N., Patwardhan, A. G., Havey, R. M., Voronov, L. I., Guo, B. Y., et al. (2007). Novel model to analyze the effect of a large compressive follower preload on range of motions in a lumbar spine. *Journal of Biomechanics, 40*(6), 1326–1332.
38. Dreischarf, M., Zander, T., Shirazi-Adl, A., Puttlitz, C. M., Adam, C. J., Chen, C. S., Goel, V. K., et al. (2014). Comparison of eight published static finite element models of the intact lumbar spine: Predictive power of models improves when combined together. *Journal of Biomechanics, 47*(8), 1757–1766.
39. Drain, O., Lenoir, T., Dauzac, C., Rillardon, L., & Guigui, P. (2008). Influence of disc height on outcome of posterolateral fusion. *Revue de Chirurgie Orthopedique et Reparatrice de L'appareil Moteur, 94*(5), 472–480.
40. Xu, M., Yang, J., Lieberman, I.H., Haddas, R. (2016). *Finite element method-based analysis for effect of vibration on healthy and scoliotic spines*. In: *Paper presented at 12th International Conference on Multibody Systems, Nonlinear Dynamics, and Control* (Vol. 6). https://doi.org/10.1115/detc2016-59679.
41. Kasra, M., Shirazi-Adl, A., & Drouin, G. (1992). Dynamics of human lumbar intervertebral joints. *Spine, 17*(1), 93–102.
42. Matsumoto, Y., & Griffin, M. J. (2002). Non-linear characteristics in the dynamic responses of seated subjects exposed to vertical whole-body vibration. *Journal of Biomechanical Engineering, 124*(5), 527.
43. Benneker, L. M., Heini, P. F., Alini, M., Anderson, S. E., & Ito, K. (2005). 2004 Young investigator award winner: Vertebral endplate marrow contact channel occlusions and intervertebral disc degeneration. *Spine, 30*(2), 167–173.
44. Gruber, H. E., Ashraf, N., Kilburn, J., Williams, C., Norton, H. J., Gordon, B. E., & Hanley, E. N. (2005). Vertebral endplate architecture and vascularization: Application of micro-computerized tomography, a vascular tracer, and immunocytochemistry in analyses of disc degeneration in the aging sand rat. *Spine, 30*(23), 2593–2600.
45. Zhu, Q., Gao, X., Brown, M. D., Chen, S., & Gu, W. (2020). Effect of intervertebral disc degeneration on mechanical and electric signals at the interface between disc and vertebra. *Journal of Biomechanics*. https://doi.org/10.1016/j.jbiomech.2020.109756.
46. Lazennec, J. Y., Ramaré, S., Arafati, N., Laudet, C. G., Gorin, M., Roger, B., et al. (2000). Sagittal alignment in lumbosacral fusion: Relations between radiological parameters and pain. *European Spine Journal, 9*(1), 47–55.
47. Schwab, F. J., Smith, V. A., Biserni, M., Gamez, L., Farcy, J. P., & Pagala, M. (2002). Adult scoliosis: A quantitative radiographic and clinical analysis. *Spine, 27*(4), 387.
48. Boissiere, L., Perrin, G., Rigal, J., Michel, F., & Barrey, C. (2013). Lumbar-sacral fusion by a combined approach using interbody PEEK cage and posterior pedicle-screw fixation: Clinical and radiological results from a prospective study. *Orthopaedics & Traumatology: Surgery & Research, 99*(8), 945–951.
49. Brinckmann, P., & Grootenboer, H. (1991). Change of disc height, radial disc bulge, and intradiscal pressure from discectomy an in vitro investigation on human lumbar discs. *Spine, 16*(6), 641–646.



**Qing-Dong Wang** received his Master degree from Northeastern University, China in 2017. He currently is a Ph.D. candidate at the School of Mechanical Engineering and Automation, Northeastern University. His research interests include Biomechanics and Mechanical CAE.

**Li-Xin Guo** received his Ph.D. at Northeastern University, China. He has been a professor at Northeastern University since 2008. He have published more than 170 research papers. His research interests include Biomechanics, Mechanical CAE, Mechanical vibration and control and Vehicle dynamics.